

Learned Image Compression for *Machine Perception*

Felipe Codevilla^{2,4}, Jean Gabriel Simard², Ross Goroshin⁵ and Chris Pal^{1,2,3,6}

¹Polytechnique Montréal, ²Mila, Quebec AI Institute ³ElementAI / Service Now,

⁴Independent Robotics, ⁵Google Brain Inc.,

⁶Canada CIFAR AI Chair,

Correspondence: felipe.alcm@gmail.com

Abstract—Recent work has shown that learned image compression strategies can outperform standard hand-crafted compression algorithms that have been developed over decades of intensive research on the rate-distortion trade-off. With growing applications of computer vision, high quality image reconstruction from a compressible representation is often a secondary objective. Compression that ensures high accuracy on computer vision tasks such as image segmentation, classification, and detection therefore has the potential for significant impact across a wide variety of settings. In this work, we develop a framework that produces a compression format suitable for both human perception and machine perception. We show that representations can be learned that simultaneously optimize for compression and performance on core vision tasks. Our approach allows models to be trained directly from compressed representations, and this approach yields increased performance on new tasks and in low-shot learning settings. We present results that improve upon segmentation and detection performance compared to standard high quality JPGs, but with representations that are **four to ten times smaller** in terms of bits per pixel. Further, unlike naive compression methods, at a level ten times smaller than standard JPEGs, segmentation and detection models trained from our format suffer only minor degradation in performance.

Index Terms—Image Compression, Computer Vision

1 INTRODUCTION

IT has been shown that image classification can be performed directly from the discrete cosine transformations used in the standard JPEG compression format, that this procedure is more computationally efficient and maintains performance comparable to state-of-the-art methods for image classification tasks [19]. In recent years a growing research community has emerged around learned image compression strategies based on deep neural networks, and many results have demonstrated that such approaches can surpass highly engineered approaches to image compression [2, 4, 34].

Neural image compression is normally formulated as an optimization balancing a trade-off between two objectives: the compression ratio and image distortion (or image quality). A common way to achieve this is to produce a representation that contains the information necessary for reconstruction while maintaining low entropy on the latent representation, under some probability model. This latent space can then be compressed to a bit-stream using a lossless compression algorithm, thus achieving a lower BPP compression of the image. In contrast, in our work here we study whether this latent space representation can be further biased or re-structured such that it better represents and retains information that is relevant for subsequent semantically oriented vision tasks such as classification, detection, and segmentation. Intuitively, our work aims to develop an approach to learning neural image compression in a way that preserves or improves performance on common machine perception tasks and yields representations that likely to retain information required when training models for *new* tasks - since the representation is explicitly learned such that it is capable of reconstructing the original image.

In our framework, these different tasks are performed by task specific decoders that operate directly on the (common) learned, compressible representation. Furthermore, we test the hypothesis that our neural compression models learned in this way might be particularly good at adapting to new tasks using a competitive low-show learning benchmark evaluation. Our approach yields state of the art performance on this evaluation. A high level view of our approach is shown in Figure 1.

We explore these ideas by biasing the learned representations of neural encoders specifically constructed to yield quantizable and compressible codes (under arithmetic coding) by jointly training them with alternative decoders for auxiliary tasks. We conjecture that this should lead to compressible representations having comparable rate/distortion characteristics while better preserving and structuring the information necessary for performing computer vision tasks directly from these highly compressible codes. We underscore that this is potentially a challenging setting, since other transfer learning work has shown that computer vision tasks such as auto-encoding and semantic segmentation can be less compatible than others, leading to decreased performance when models are trained on both tasks simultaneously [50].

The contribution of our work here is to propose and explore a joint training procedure that allows models to learn highly compressible representations, while minimizing the impact on performance on key machine perception tasks. Importantly, in our approach these tasks are performed directly from the compressed representation, without the need for decoding the image. We test our hypothesis that this approach might yield representations that are well suited for

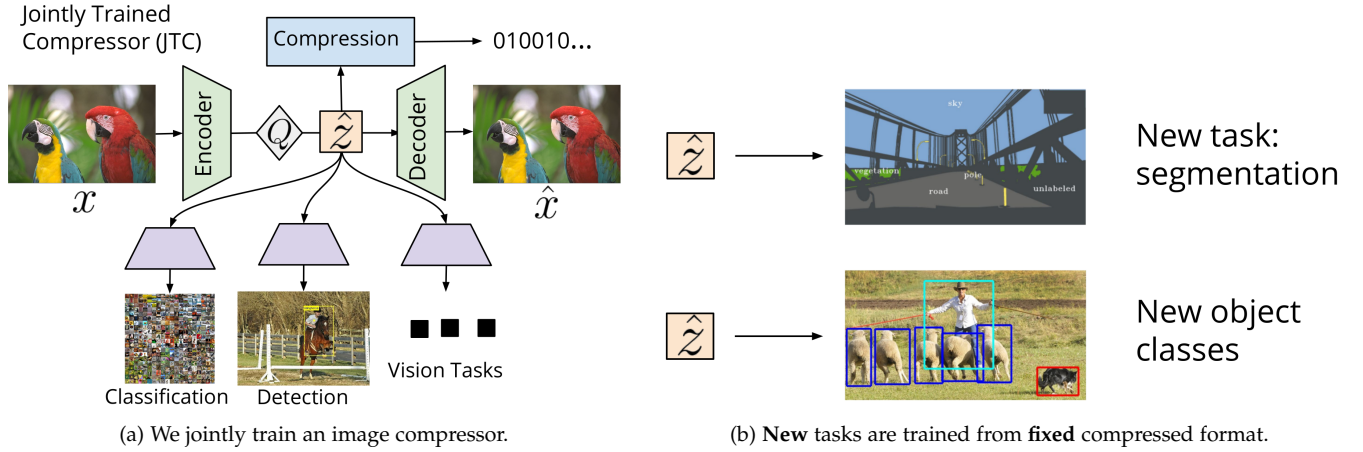


Fig. 1: A high level view of our strategy for learning compressible image representations for machine perception. We jointly train a model to compress as well as perform key vision tasks directly from the compressible representation. The approach leads to significant gains compared to both JPEG or naive learned deep compression when training new models for new tasks directly from our learned compressible representations.

new tasks and few-shot learning. We find that they achieve state-of-the-art performance on few-shot image detection when learning directly from our task-informed compressible representations. Furthermore, our representations can be compressed to be *four to ten times smaller than standard JPEG imagery* while improving performance or suffering only a minor degradation on the key vision tasks of classification, detection and segmentation.

2 LEARNING COMPRESSIBLE REPRESENTATIONS FOR MACHINE PERCEPTION TASKS

2.1 Preliminaries: Rate-Distortion and Perceptual Quality

The traditional goal of lossy image compression is to find the best trade-off between minimizing the expected length of the bit-stream representing the input image, x , and minimizing the expected distortion between the image and its reconstruction \hat{x} . In the information theory literature, this is known as the rate-distortion optimization problem [13]. In the context of learned image compression, this can be formulated as a multi-task loss:

$$\mathcal{R}(\mathbf{Q}(f(x))) + \lambda \cdot \mathcal{D}(g(\mathbf{Q}(f(x))), x), \quad (1)$$

where \mathcal{R} represents the rate or bit-stream length, and \mathcal{D} represents the distortion or reconstruction fidelity, usually implemented by a distance function. To find such an encoding, the non-linear transform coding strategy [18] consists of producing a discrete latent representation z from an image x using an *encoder*, i.e. $z = f(x)$. This real-valued representation is quantized, by a quantization operator \mathbf{Q} , into \hat{z} . The reconstructed input, \hat{x} , is generated by the image decoder $g(\hat{z})$. Because both objectives cannot be completely minimized simultaneously, different values of λ lead to a different operating points in the trade-off between rate and distortion. Note that the representation \hat{z} must be an element of a finite set to be losslessly encoded to a bit-stream with a lossless compression algorithm such as arithmetic coding [30]. Because perceptual quality is not directly correlated with distortion, a perceptual quality metric is often

added to the loss [7]. This idea has been used to improve the quality of image compression algorithms [33].

2.2 Rate-Distortion-Utility Perspective

The representation z can be encoded in a bit stream and stored or transmitted, but also used directly to perform visual tasks *without reconstructing* the input image [45]. This common use-case highlights the potential of exploring another dimension beyond the classical rate-distortion optimization trade-off. Rather than thinking of perceptual quality as the difference between reconstructed and the original images, we are interested in the direct utility of the learned compressed representation for machine perception tasks.

This leads to our *key hypothesis*: For any desired rate, R , and distortion level D , we conjecture that there exists many different, quantized latent representations, $\hat{z} = \mathbf{Q}(f(x))$, which lead to significant differences in performance on subsequent machine vision tasks. In other words, there exists many representations which achieve a given rate-distortion trade-off, but some representations may be better suited for subsequent semantic tasks than others.

In this context, we propose that the objective function to be optimized should go beyond the classical rate-distortion paradigm, to include a measure of the utility of the representation for concrete machine perception tasks:

$$\mathcal{R}(\mathbf{Q}(f(x)), x) + \lambda_d \cdot \mathcal{D}(g(\mathbf{Q}(f(x))), x) + \lambda_u \cdot \mathcal{U}(\mathbf{Q}(f(x))), \quad (2)$$

where $\mathcal{U}(\cdot)$ is a pragmatically defined utility, or machine perceptual quality metric. In contrast to the usual notion of human perceptual quality which is often characterized by metrics such as squared error, we can define machine vision perceptual quality much more pragmatically, i.e. based on a multi-task loss:

$$\mathcal{U}(\mathbf{Q}(f(x))) = \sum_{t \in \mathcal{T}} \lambda_t [L_t(h_t(f(x)), y_t)], \quad (3)$$

where L_t is a loss function for an specific task t with respect to the labels y_t . The functions h_t are the task specific

decoders. We conjecture that the optimization of learned compression models for rate \mathcal{R} , distortion \mathcal{D} , and utility \mathcal{U} as defined in (2) will result in encoders $f(x)$ that are capable of producing low bit-per-pixel quantized representations \hat{z} that are better structured to facilitate the learning of new machine perception tasks directly from \hat{z} .

2.3 Compression Architecture

We base our image compression approach on the hierarchical variational-auto-encoder (VAE) formulation proposed by [5]. The function \mathcal{R} is computed as the expected marginal probability of the latent *quantized* representation, $\mathbb{E}[-\log_2 p_z(\hat{z})]$, where \hat{z} is a the quantized encoding of an input image and the expectation is with respect to the empirical distribution of a training set. A Gaussian Mean-Scale Model (GMSM) is used for $p_z(\hat{z})$ as suggested in [5, 34]. Each element of \hat{z} is modeled by a Gaussian with a mean and a unique scale for a given lossless compression ratio.

Since quantization is not a differentiable operation, a special form of uniform noise is added to the latent variables z during training, which yields a differentiable strategy in which one must ensure that the amplitude of the noise keeps the codes within the same quantization bin. This induces the encoder to learn to output a code that is invariant to integer quantization. Recall that the addition of two independent random variables follows the convolution of their individual distributions. Therefore, the addition of uniform noise to the latent representation leads to a model of the form:

$$p_z(\hat{z}) = \prod_i \left(\mathcal{N}(\mu_i, \sigma_i) * u\left(-\frac{1}{2}, \frac{1}{2}\right) \right) (\hat{z}_i), \quad (4)$$

where all the elements of $p_z(\hat{z})$ are independent and ‘*’ denotes the convolution operator. The values of μ_i and σ_i are the mean and variances output by the *hyper-prior* network comprised of a separate VAE which encodes the latent representation z into the quantized hyper-parameter \hat{w} and decodes it into the parameters of the probabilistic model p_z . See Appendix I for further details.

We use a mean squared error distortion metric, which results in the following loss function for our naive (i.e. in that it is not task informed) compression framework:

$$\mathbb{E}[-\log_2 p_z(\hat{z})] + \mathbb{E}[-\log_2 p_{\hat{w}}(\hat{w})] + \lambda \mathbb{E}[\|x - g(\hat{z})\|^2], \quad (5)$$

where $\mathbb{E}[-\log_2 p_z(\hat{z})]$ is the expected compression rate of the latent representation \hat{z} and $\mathbb{E}[-\log_2 p_{\hat{w}}(\hat{w})]$ the expected compression rate of the hyper-latent representation \hat{w} . The loss corresponding to our task informed compression setup is obtained by combining the multi-task loss from (3) and using our rate-distortion-utility framework to obtain our task informed learned compression optimization framework:

$$\mathbb{E}[-\log_2 p_z(\hat{z})] + \mathbb{E}[-\log_2 p_{\hat{w}}(\hat{w})] + \lambda_e \mathbb{E}[\|x - g(\hat{z})\|^2] + \sum_{t \in \mathcal{T}} \lambda_t \mathbb{E}[L_t(h_t(\hat{z}), y_t)]. \quad (6)$$

2.4 A Multi-task Inference and Compression Architecture

Here we illustrate the architecture, $h(z)$, used to produce results for different vision tasks. The same architecture is used both to optimize for the machine perception quality and perform inference from the compressible representation.

A detailed visualization of our proposed architecture is depicted in Figure 2. The compression architecture is depicted at the top of the figure (encoder/decoder). This architecture is the same as proposed by [10]. The encoder is composed of four convolutional layers interlaced by so-called Generalized Divisive Normalization (GDN) layers [3] for activation. The encoder expects an RGB image of size $3 \times W \times H$ and outputs a tensor of shape $256 \times W/16 \times H/16$. Note, the rank of the compressible format is one third of the input image rank, but is actually smaller still (in bpp) because of its redundancy. In order to perform vision tasks directly from the latent space, it is necessary to adapt the backbone ResNet architecture, commonly used to extract useful features for vision tasks. Compared to the original image, the input is comprised of many channels with lower spatial resolution. Several solutions have been proposed to this problem. In [19], the authors observed that a learned deconvolution yields better results since it helps overcoming the reduction in receptive field. In [45], the authors proposed to simply remove the the first layers of a Resnet and input the compressed space as is. This inputs the latent space directly to the first Resnet bottleneck block, which does not allow a space with bigger receptive field to be included.

Here we observed the necessity of recovering the full image resolution and propose a pixel shuffle adapter that outputs directly to the bottleneck blocks of the Resnet. It was observed in [45], especially for lower bit rate configurations, a notable loss in performance for tasks that require spatial information such as semantic segmentation. Pixel shuffle [41] performs sub-pixel resolution convolutions and mitigates any potential loss of spatial information. The architecture, refereed as *sResnet* is depicted Fig. 2, and contains three convolutional blocks (which include ReLUs) interlaced with two pixel shuffle blocks. A complete detailed description of the architecture is presented in the supplementary material.

3 EXPERIMENTAL RESULTS AND DISCUSSION

We investigate the potential of performing classification, object detection, few-shot detection and segmentation directly from the different, previously described, informed compressible representations and how well this information generalizes to new tasks and categories. In other words, we investigate whether compression formats can be biased to preserve semantic information. First, we study compression performance and show that our approach is on-par with known state-of-the art CNN-based models and exceeds the performance of popular compression algorithms. We examine the impact of adding different decoder networks trained to perform computer vision tasks directly from our compressible representation. This includes training directly from compressible codes for semantic segmentation, a held-out task not used to train the representation. We also provide an ablation analysis and examine different model variants. We then explore this approach for learning low shot object

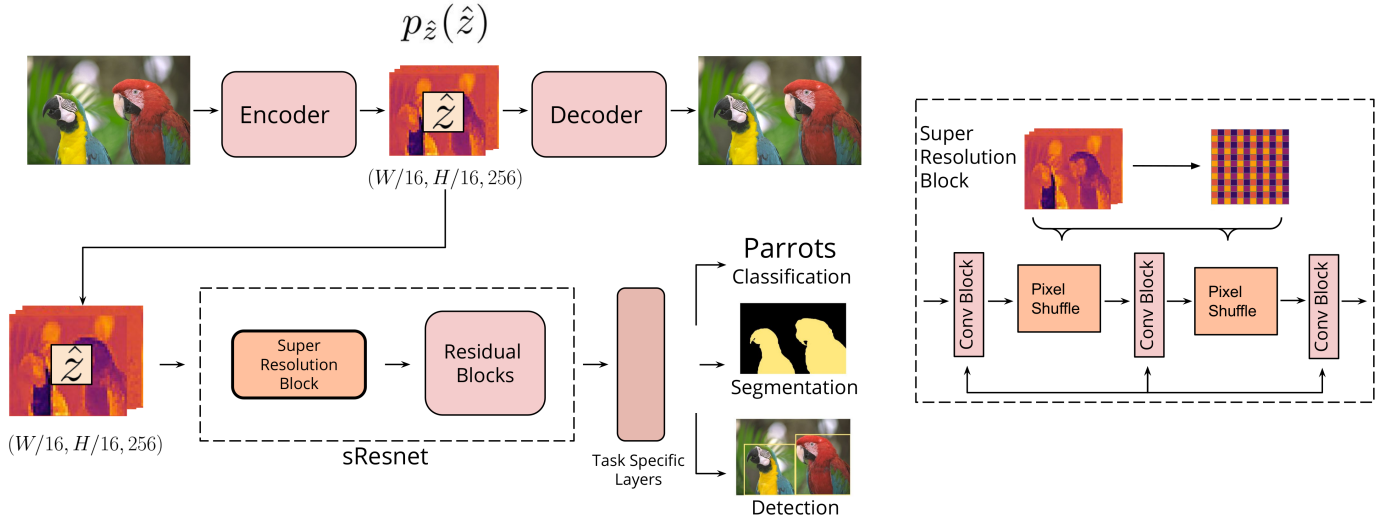


Fig. 2: Detailed architecture of the proposed model for jointly training of image compression with different computer vision tasks.

detection. Finally, we examine questions of computation efficiency.

3.1 Visual Results and Implementation Details for Learning Compressed Representations

In Figure 3 we show the results of our proposed rate-distortion-utility approach to learned compression in panels (d) and (e). We compare it with JPEG compression at a much higher bitrate of 0.31 bpp, in (c) and a naive version of our approach in (b) – which one could consider as an instance of, or comparison with the approach proposed in [5], but implemented within a specific encoder architectures held fixed across these experiments. The architecture is the best one from the broader family of neural compression models discussed and explored in more detail below. Notice that we can see a striking phenomenon: at very high λ_t , the texture on an object category of interest to the classifier/detector (a bird in this case) is preserved while the background (foliage) is compressed. This is in agreement with the recent finding that convolutional networks tend to focus on texture rather than shape [21].

We obtain a compressible space z to perform vision tasks by applying Equation (6) over the datasets detailed below. For all our experiments we use the Adam optimizer with an initial learning rate of 5×10^{-5} . The training dataset used to train the image decoder is a subset of 400k images of OpenImages [29] that was pre-processed using the strategy proposed by [32] that downscales the images in order to reduce potential compression artifacts. To test compression quality results, we use the standard losslessly compressed Kodak dataset [28]. We use classification and detection losses to approximate a machine perception quality metric. Differently from [45], we train on the compression and the machine perception tasks from scratch, jointly. For classification, we use multi-class cross-entropy as the loss function. We train the model using the ImageNet dataset jointly with OpenImages [29]. We train both tasks for 70 epochs dividing the learning rate by a factor of 10 every 30 epochs. In order to sample the same number of images for

each task (reconstruction and classification) we set a batch size of 72 for image reconstruction, which is substantially bigger than the batch size used in previous work [5]. For the classification task we set a batch size of 256. Jointly trained with classification we experiment with two **class informed** models. We set $\lambda_t = 10, \lambda_d = 100$ to obtain a bit-rate of ≈ 0.4 , $\lambda_t = 10, \lambda_d = 10$ for a bit-rate of ≈ 1.0 . For detection, the task specific module in this case consist of an architecture based on a Faster-RCNN [37] structured module, which contains a region proposal network and bounding box classifier. We use Pascal VOC as the training dataset. Finally, the standard region-proposal regression and detection class loss [37] are used as the detection loss function. We built two **detection informed** models. We set $\lambda_t = 100, \lambda_d = 100$ to obtain a bit-rate of ≈ 0.4 , $\lambda_t = 100, \lambda_d = 25$ for a bit-rate of ≈ 1.0 . We also trained **class and detection informed model** with a bit-rate of ≈ 1.0 using $\lambda_t = 5$ for classification $\lambda_t = 100$ for detection and $\lambda_d = 25$. All the λ hyper-parameters were chosen in order to balance the different batch sizes of tasks.

3.2 Evaluating Our Learned Compression Approach

We evaluate different strategies for learning informed compressible representations on various downstream tasks. For all tasks, the size of the input compressible representation is of $256 \times W/16 \times H/16$. We assume a fully-trained input representation capable being decoded back to the input RGB image; and capability to encode a bitstream from the latent space. In practice the second requirement means that the latent representation is invariant to quantization for the purpose of reconstruction. For all cases, we use the sResnet architecture with a ResNet-101 backbone. We added task specific layers, accordingly, for each task.

Classification. We investigate the classification accuracy on the ImageNet validation set while training in the full ImageNet dataset 2012 [40]. We use the default hyper-parameters used for training a Resnet architecture [20]. This includes, stochastic gradient descent as optimizer and a

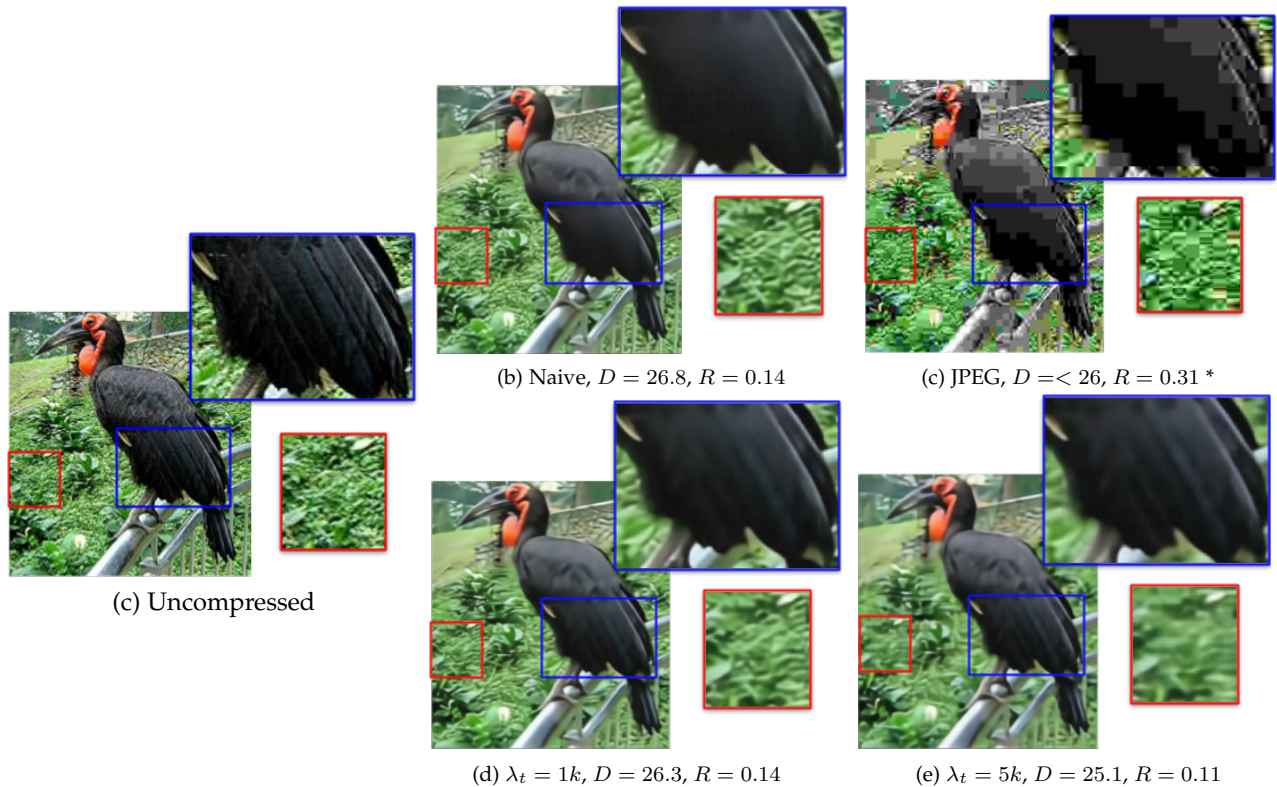


Fig. 3: Visual image quality comparisons, at distortion level D (PSNR), and rate R (bpp). (a) Uncompressed ground-truth (b) Naive hyper-prior based learned compressor. (c) JPEG compressed image. (d)-(e) Compressor jointly trained with an object detector using the λ_t parameters, respectively, as 1000 and 5000. We observe that increasing the importance of Pascal object detection performance (i.e. the Utility U of the representation) improves the visual quality of the texture features on the birds feathers and reduces the quality of the background (foliage).

starting learning rate of 0.1 that is divided by 10 every 30 epochs. We also set the batch size as 256 for training.

Detection. We also investigate the average precision on a detection task using the Faster-RCNN [38] region proposal and classification heads. Similarly to segmentation, we initialize the training with ImageNet weights trained for the compressed representation.

Semantic Segmentation. For this task specific module we use the Deep Lab V3 [9] and an atrous spatial pyramid pooling layer. We train and evaluate a semantic segmentation network on the Pascal VOC dataset [15], measuring the mean intersection over union (mIoU) score. It is important to note that competitive semantic segmentation results can only be obtained when starting from backbone weights that were pre-trained on ImageNet, we found this also to be the case when training from compressible representations. Therefore we initialize training for the semantic segmentation task with the sResNet-101 weights learned by the classification task.

The results when given different representation inputs for training are presented on Table 1. The main feature we observe is the capability to improve over the results of an uncompressed input by using a compressible representation that is five times smaller. The uncompressed baselines were trained with the JPEG image set provided on the ImageNet, for classification, and the PascalVOC datasets, for detection and semantic segmentation. We observe the overall best performance on semantic segmentation and image detection,

when using our compression trained with classification and detection features. This is an interesting boost and proves the generality of our method since no features from semantic segmentation were used when training the compressed representation input. Those results corroborate our hypothesis that constraining the representation learning problem into also being a compressible representation aids generalization. Also, it is important to notice that, for segmentation and detection, that the classification and detection informed results perform better than only detection or only classification informed compressed formats. This indicates that increasing the amount of information for the compressed representation may improve generalization performance.

We can perceive an even clearer benefit when training from compressed representations when the compression rate (bits/pixels) is larger. The image classification results obtained for low compression, 0.4 bpp, fourth row on Table 1, are able to match the results obtained for mid compression, 1.0 bpp. That indicates a clearer benefit of using informed compressed spaces in lower bit-rate regimes. As a drawback, we see that the improvement by using informed compressed representations for classification is limited, not being able to fully recover the uncompressed classification results. An insight into these results can be acquired by observing the reconstruction of some informed compressed representations on Fig.3 (e) where, even though the bit rate is lower, the features of the object of interest are well maintained.

Rate	Input	Distortion	Segmentation*	Classification		Detection	
		PSNR	mIoU	Top 1	Top 5	mAP	AP50
	RGB from standard 4 to 5 bpp JPEGs		70.8	77.3	93.3	53.1	80.8
1.0 bpp \sim	RGB from 1 bpp JPEGs	32.0	67.5	75.0	92.2	52.3	79.8
	Our Compression - Naively Learned	36.2	67.5	74.8	92.2	52.8	80.3
	Our Compression - Class Informed	34.6	69.5	75.1	92.4	54.7	81.1
	Our Compression - Detection Informed	35.6	70.5	74.9	92.1	54.4	81.4
	Our Compression - Class & Detection Informed	34.5	71.3	75.1	92.2	54.6	81.6
0.4 bpp \sim	RGB from .4 bpp JPEGs	28.0	57.8	70.7	89.8	51.4	78.1
	Our Compression - Naive Learned	30.7	68.9	74.0	91.7	52.1	79.6
	Our Compression - Class Informed	30.1	69.0	75.1	92.3	52.8	80.1
	Our Compression - Detection Informed	30.5	70.2	74.8	92.1	52.9	80.3

TABLE 1: Comparison of task performance when using different compressible latent formats as input. Classification experiments are on ImageNet, while Detection and Segmentation experiments are on the Pascal VOC. *Note that none of our learned compressed representations were trained for semantic segmentation; however, a model trained from our best 1bpp compressed representation can even outperform training from high quality RGB images (**bold green**). Importantly, recall that the encoder is frozen and learning is performed directly from our compressed format.

3.3 Ablations and Analysis

Table 2 shows the impact that different architectural elements have on training with compressed representations as input. Those differences are compared based on the Top 1 classification result on the ImageNet validation set. We can see that increasing the number of pixel shuffle blocks has a substantial positive impact on the results. The same is true when adding a residual connection. We also observed some considerable improvements when using the Mish [36] or the SiLU [14] activation functions as compared to the standard ReLU activations.

In Table 3 we show the comparison our super-resolution based architecture with the one proposed by [45]. A significant impact on the results can be observed, particularly on the classification task. We believe that this is likely due to a better initial receptive field being presented to the ResNet backbone. We can also see the benefit of using a task informed representation both for the simpler architecture (cResnet) and the one proposed (sResNet).

3.4 New Object Detection Categories in the Low-shot Learning Regime

The jointly trained compressed representations are particularly interesting for low-shot regimes. We conduct experiments on few-shot detection by reproducing the experiments and evaluation procedure in [47] using their open source code base. The dataset used is Pascal VOC, and Faster-RCNN as the detector architecture [38]. The classes are separated into 15 base classes and 5 novel classes. First, the detector is trained on the 15 base classes. Then, in the fine-tuning phase, the detector learns a new bounding-box (bbox) classifier and a new bbox regressor using only $k \in \{1, 2, 3, 5, 10\}$ samples from the base classes and the novel classes. The results of our experiments are summarized on Table 4. For all the compressed representations we use a bit rate of 1 bpp.

These experiments show that training the few-shot detector from our classification informed compressible representation not only improves overall few-shot performance

at 1 bpp, but also achieves state-of-the-art results for many of the experimental configurations. Also, note that the addition of semantic information to the representation has a significant impact, leading to an average increase of 4 points in mAP50. This strongly suggests that, when jointly trained with visual tasks, compressible representations can serve as a regularizer in low-data regimes. Finally, the performance gap between our method and the TFA method [47] is even larger when the compression level is increased on the TFA input to match a bit rate of 1.0.

3.5 Computational and Memory Cost

All the performance benchmarks were made on 4 Nvidia V100 GPUs processing a batch in parallel. One of the motivations for our approach is the fact that there exists an advantage to performing downstream tasks directly from a latent compressed space, besides the obvious saving storage/transmission requirement, the input size is considerably smaller and thus computationally cheaper to forward propagate (fprop). We typically see performance gains of up to 20% on the classification task. However, it should be noted that our experiments are performed at full 32-bit floating point resolution, yet the compressible representation can be expressed using 4-bits. See Appendix I for more details. The use of 4-bit representations for our compression format could make data processing pipelines even more efficient. Furthermore, if combined with appropriately engineered low-bit decoders we suspect that much more dramatic computational gains are possible for those who desire improved performance in this regard. Given that the field of low bit precision deep learning has been making many advances [6, 12, 24, 25], low-bit depth decoders based on this type of compression scheme could be an interesting direction for future work. A recent survey in [17] summarizes some key developments, including extremely fast INT8 and INT4 implementations of canonical Convolutional Neural Network architectures.

One pixel shuffle block	Two pixel shuffle blocks	Residual block	Mish	SiLU	Top 1
✓					69.2
✓		✓			71.2
	✓	✓			74.8
	✓	✓	✓		75.0
	✓	✓		✓	75.1

TABLE 2: Ablation analysis and architecture variant comparisons for the classification task.

Input	Segmentation mIoU	Classification		Detection	
		Top 1	Top 5	mAP	AP50
RGB from standard 4 to 5 bpp JPGs	70.8	77.3	93.3	53.1	80.8
cResnet (0.4 bpp) [45]	64.39	70.34	89.75	-	-
cResnet Detection Informed (0.4 bpp)	64.82	71.57	90.47	-	-
sResnet (0.4 bpp)	68.9	74.0	91.7	52.1	79.6
sResnet Detection Informed (0.4 bpp)	70.2	75.1	92.3	52.9	80.3

TABLE 3: Ablation analysis and comparison of different architectural variants for creating compressed representations on different downstream tasks at low bit-per-pixels.

Method	# of Training Examples	→	Novel Set 1					Novel Set 2					Novel Set 3				
			1	2	3	5	10	1	2	3	5	10	1	2	3	5	10
MetaDet [48]			18.9	20.6	30.2	36.8	49.6	21.8	23.1	27.8	31.7	43.0	20.6	23.9	29.4	43.9	44.1
Meta R-CNN [49]			19.9	25.5	35.0	45.7	51.5	10.4	19.4	29.6	34.8	45.4	14.3	18.2	27.5	41.2	48.1
TFA w/fc [47]			36.8	29.1	43.6	55.7	57.0	18.2	29.0	33.4	35.5	39.0	27.7	33.6	42.5	48.7	50.2
TFA w/cos [47]			39.8	36.1	44.7	55.7	56.0	23.5	26.9	34.1	35.1	39.1	30.8	34.8	42.8	49.5	49.8
TFA w/fc, our compression			35.6	27.4	42.8	54.2	55.6	16.3	28.0	31.9	33.9	37.8	25.0	31.5	40.6	47.0	48.4
Ours - Naive			33.5	26.3	40.7	53.5	55.1	20.2	24.1	30.5	31.1	36.8	26.1	30.5	38.7	45.6	45.9
Ours - Class. + Det. Informed			38.1	37.3	44.7	56.2	57.1	23.6	27.3	34.0	35.1	38.9	31.0	33.9	42.1	48.7	48.9
Ours - Classification Informed			38.8	37.2	44.1	55.3	56.7	23.7	27.2	34.5	35.3	39.2	31.2	34.9	42.5	49.4	49.5
Ours - Detection Informed			39.3	37.5	44.8	56.3	57.1	23.7	29.1	34.8	35.3	39.2	31.3	34.9	42.9	49.5	49.9

TABLE 4: Few-shot detection performance (mAP50) on PASCAL VOC dataset. We compare our results (bottom) when using a informed compressed representation with other methods from the literature. We obtain a convincingly better performance while using a mid bit-rate representation (bpp 1.0).

4 RELATED WORK

Early work using auto-encoder architectures for image compression date back to the late 1980’s [11] and many extensions were developed during the following decades [26]. They follow the traditional approach of pixel transforms, quantization, and entropy coding. The use of recurrent architectures [27, 44] was proposed to allow configurable rate-distortion trade-off by progressively encoding image residuals, this can also be improved by tiling [35].

Most relevant to our work, is the state-of-the-art technique of creating a latent representation using a variational auto-encoder and using a hyper-prior network to produce a probabilistic model of the quantized latent representation [5, 10, 34]. We use the quantized latent space of the VAE as an input format for visual tasks, thus the latent space should capture all necessary information for performing these tasks. Those techniques have also been recently extended to include perceptual quality metrics, drastically improving the results from a human perception perspective [1, 33]. The present work does not focus on improving results from a distortion or human perception viewpoint, but strives to improve the compression format for machine perception via canonical computer vision tasks such as image classification or object detection as proxies.

Recent work has shown that it is possible to learn compressible representations of features in deep neural networks that do not reconstruct input images [43], but which serve to perform classifications. Their work shows that it is possible to create image classifiers using the resulting

compressed feature representations that have comparable performance to those trained directly on images. At the other end of the spectrum, as mentioned in our introduction, other work has used the image representations obtained from the ubiquitous JPEG image compression format as input to convolutional networks. This approach reduces the computational and memory requirements of the overall pipeline of training and classification while achieving a similar accuracy on ImageNet classification [16, 19, 46].

We also propose the approach of performing tasks directly from compressible representations; however, the aim of our work is to *learn a semantically sensitive compressible image format* which facilitates downstream tasks such as classification and semantic segmentation. Of course there is considerable prior work that has involved training auto-encoders to learn image features via low-dimensional embeddings or codes [23] [31]. However, these types of approaches have not involved explicitly compressing the latent representations and evaluating such methods in terms of compression rates and distortion. In contrast, our approach and architectures produce low dimensional feature spaces with reduced entropy through encouraging representations to be robust to the integer quantization necessary for arithmetic coding. This approach thereby leads to measurable gains in yielding compressible image representations.

Because image reconstruction and other semantic tasks can be viewed as competing objectives, our work is highly related to multi-task learning [39]. To the best of our knowledge the work most closely related to ours is [45], which

was the first to perform semantic inference directly from a learned, compressible representation. However, in their work performance was compromised on semantic tasks. We also explore inference from a compressible representation, however we aim to develop an algorithm that produces *semantically sensitive compressible representations without sacrificing their ability to compute the information necessary to reconstruct the input image*. Our experiments underscore the various advantages of our proposed format, particularly when learning new out-of-domain tasks and for few-shot generalization.

5 CONCLUSIONS

We have proposed stepping away from the classical rate-distortion paradigm for learned image compression and moving to a rate-distortion-utility framework. We have shown that this can be achieved by simply jointly training a compressor to also serve as the intermediate representation for multiple tasks. Our work provides evidence that the combined effects of: (1) compact codes provided by explicit neural compression techniques, and (2) a multi-task learning setup, indeed produces representations that are particularly effective in both: (a) the low shot learning regime, and (b) when training a new task such as semantic segmentation directly from these types of learned compressed representations for machine perception. It should be noted that encouraging compression methods to better preserve certain types of semantic content could introduce biases into which elements of an image are better compressed than others. One must therefore ensure that unwanted biases are not unintentionally induced in the algorithm. If our approach becomes adopted, as time goes on even larger datasets of tasks could address the limitations of training using only the ImageNet, OpenImages and Pascal datasets.

ACKNOWLEDGMENTS

We thank NSERC, the COHESA Strategic Network, Google, Mila and CIFAR for their support under the AI Chairs program.

REFERENCES

- [1] Eirikur Agustsson, Michael Tschannen, Fabian Mentzer, Radu Timofte, and Luc Van Gool. Generative adversarial networks for extreme learned image compression. In *Proceedings of the IEEE/CVF International Conference on Computer Vision*, pages 221–231, 2019.
- [2] Eirikur Agustsson, Michael Tschannen, Fabian Mentzer, Radu Timofte, and Luc Van Gool. Generative Adversarial Networks for Extreme Learned Image Compression. 2018.
- [3] Johannes Ballé, Valero Laparra, and Eero P. Simoncelli. Density modeling of images using a generalized normalization transformation. *ICLR*, pages 1–14, 2016.
- [4] Johannes Ballé, David Minnen, Saurabh Singh, Sung Jin Hwang, and Nick Johnston. Variational image compression with a scale hyperprior. *ICLR*, 2018.
- [5] Johannes Ballé, David Minnen, Saurabh Singh, Sung Jin Hwang, and Nick Johnston. Variational image compression with a scale hyperprior. *arXiv preprint 1802.01436*, 2018.
- [6] Ron Banner, Itay Hubara, Elad Hoffer, and Daniel Soudry. Scalable methods for 8-bit training of neural networks. In *NeurIPS*, 2018.
- [7] Yochai Blau and Tomer Michaeli. Rethinking lossy compression: The rate-distortion-perception tradeoff. *arXiv preprint arXiv:1901.07821*, 2019.
- [8] Matteo Carandini and David J Heeger. Normalization as a canonical neural computation. *Nature Reviews Neuroscience*, 13(1):51–62, 2012.
- [9] Liang-Chieh Chen, George Papandreou, Florian Schroff, and Hartwig Adam. Rethinking atrous convolution for semantic image segmentation. *arXiv preprint arXiv:1706.05587*, 2017.
- [10] Zhengxue Cheng, Heming Sun, Masaru Takeuchi, and Jiro Katto. Learned image compression with discretized gaussian mixture likelihoods and attention modules. In *Proceedings of the IEEE/CVF Conference on Computer Vision and Pattern Recognition*, pages 7939–7948, 2020.
- [11] Garrison W. Cottrell. Image compression by back propagation: an example of extensional programming. 1988.
- [12] Matthieu Courbariaux, Yoshua Bengio, and Jean-Pierre David. Binaryconnect: training deep neural networks with binary weights during propagations. In *Proceedings of the 28th International Conference on Neural Information Processing Systems-Volume 2*, pages 3123–3131, 2015.
- [13] Thomas M Cover. *Elements of information theory*. John Wiley & Sons, 1999.
- [14] Stefan Elfving, Eiji Uchibe, and Kenji Doya. Sigmoid-weighted linear units for neural network function approximation in reinforcement learning. *Neural Networks*, 107:3–11, 2018.
- [15] Mark Everingham, Luc Van Gool, Christopher KI Williams, John Winn, and Andrew Zisserman. The pascal visual object classes (voc) challenge. *International journal of computer vision*, 88(2):303–338, 2010.
- [16] Dan Fu and Gabriel Guimaraes. Using compression to speed up image classification in artificial neural networks, 2016.
- [17] Amir Gholami, Sehoon Kim, Zhen Dong, Zhewei Yao, Michael W Mahoney, and Kurt Keutzer. A survey of quantization methods for efficient neural network inference. *arXiv preprint arXiv:2103.13630*, 2021.
- [18] Vivek K Goyal. Theoretical foundations of transform coding. *IEEE Signal Processing Magazine*, 18(5):9–21, 2001.
- [19] Lionel Gueguen, Alex Sergeev, Ben Kadlec, Rosanne Liu, and Jason Yosinski. Faster neural networks straight from jpeg. In *Advances in Neural Information Processing Systems*, pages 3933–3944, 2018.
- [20] Kaiming He, Xiangyu Zhang, Shaoqing Ren, and Jian Sun. Deep residual learning for image recognition. In *Proceedings of the IEEE conference on computer vision and pattern recognition*, pages 770–778, 2016.
- [21] Katherine L Hermann, Ting Chen, and Simon Kornblith. The origins and prevalence of texture bias in convolutional neural networks. *arXiv preprint*

- arXiv:1911.09071*, 2019.
- [22] Irina Higgins, Loic Matthey, Arka Pal, Christopher Burgess, Xavier Glorot, Matthew Botvinick, Shakir Mohamed, and Alexander Lerchner. beta-vae: Learning basic visual concepts with a constrained variational framework. *ICLR*, 2017.
- [23] Geoffrey E Hinton and Ruslan R Salakhutdinov. Reducing the dimensionality of data with neural networks. *science*, 313(5786):504–507, 2006.
- [24] Itay Hubara, Matthieu Courbariaux, Daniel Soudry, Ran El-Yaniv, and Yoshua Bengio. Binarized neural networks. In *Proceedings of the 30th International Conference on Neural Information Processing Systems*, pages 4114–4122, 2016.
- [25] Forrest N Iandola, Song Han, Matthew W Moskewicz, Khalid Ashraf, William J Dally, and Kurt Keutzer. Squeezenet: Alexnet-level accuracy with 50x fewer parameters and; 0.5 mb model size. *arXiv preprint arXiv:1602.07360*, 2016.
- [26] J Jiang. Image compression with neural networks—a survey. *Signal processing: image Communication*, 14(9):737–760, 1999.
- [27] Nick Johnston, Damien Vincent, David Minnen, Michele Covell, Saurabh Singh, Troy Chinen, Sung Jin Hwang, Joel Shor, and George Toderici. Improved lossy image compression with priming and spatially adaptive bit rates for recurrent networks. In *Proceedings of the IEEE Conference on Computer Vision and Pattern Recognition*, pages 4385–4393, 2018.
- [28] Eastman Kodak. Kodak lossless true color image suite (photocd pcd0992). URL <http://r0k.us/graphics/kodak>, 1993.
- [29] Alina Kuznetsova, Hassan Rom, Neil Alldrin, Jasper Uijlings, Ivan Krasin, Jordi Pont-Tuset, Shahab Kamali, Stefan Popov, Matteo Mallocci, Tom Duerig, et al. The open images dataset v4: Unified image classification, object detection, and visual relationship detection at scale. *arXiv preprint arXiv:1811.00982*, 2018.
- [30] Glen G Langdon. An introduction to arithmetic coding. *IBM Journal of Research and Development*, 28(2):135–149, 1984.
- [31] Jonathan Masci, Ueli Meier, Dan Cireşan, and Jürgen Schmidhuber. Stacked convolutional auto-encoders for hierarchical feature extraction. In *International conference on artificial neural networks*, pages 52–59. Springer, 2011.
- [32] Fabian Mentzer, Eirikur Agustsson, Michael Tschanen, Radu Timofte, and Luc Van Gool. Practical full resolution learned lossless image compression. In *Proceedings of the IEEE Conference on Computer Vision and Pattern Recognition*, pages 10629–10638, 2019.
- [33] Fabian Mentzer, George D Toderici, Michael Tschanen, and Eirikur Agustsson. High-fidelity generative image compression. *Advances in Neural Information Processing Systems*, 33, 2020.
- [34] David Minnen, Johannes Ballé, and George Toderici. Joint autoregressive and hierarchical priors for learned image compression. *Advances in Neural Information Processing Systems*, 2018-December(Nips):10771–10780, 2018.
- [35] David Minnen, George Toderici, Michele Covell, Troy Chinen, Nick Johnston, Joel Shor, Sung Jin Hwang, Damien Vincent, and Saurabh Singh. Spatially adaptive image compression using a tiled deep network. In *2017 IEEE International Conference on Image Processing (ICIP)*, pages 2796–2800. IEEE, 2017.
- [36] Diganta Misra. Mish: A self regularized non-monotonic activation function. *arXiv preprint arXiv:1908.08681*, 2019.
- [37] Shaoqing Ren, Kaiming He, Ross Girshick, and Jian Sun. Faster r-cnn: Towards real-time object detection with region proposal networks. *arXiv preprint arXiv:1506.01497*, 2015.
- [38] Shaoqing Ren, Kaiming He, Ross Girshick, and Jian Sun. Faster r-cnn: Towards real-time object detection with region proposal networks, 2016.
- [39] Sebastian Ruder. An overview of multi-task learning in deep neural networks. *arXiv preprint arXiv:1706.05098*, 2017.
- [40] Olga Russakovsky, Jia Deng, Hao Su, Jonathan Krause, Sanjeev Satheesh, Sean Ma, Zhiheng Huang, Andrej Karpathy, Aditya Khosla, Michael Bernstein, et al. Imagenet large scale visual recognition challenge. *International journal of computer vision*, 115(3):211–252, 2015.
- [41] Wenzhe Shi, Jose Caballero, Ferenc Huszár, Johannes Totz, Andrew P Aitken, Rob Bishop, Daniel Rueckert, and Zehan Wang. Real-time single image and video super-resolution using an efficient sub-pixel convolutional neural network. In *Proceedings of the IEEE conference on computer vision and pattern recognition*, pages 1874–1883, 2016.
- [42] Wenzhe Shi, Jose Caballero, Ferenc Huszár, Johannes Totz, Andrew P. Aitken, Rob Bishop, Daniel Rueckert, and Zehan Wang. Real-time single image and video super-resolution using an efficient sub-pixel convolutional neural network, 2016.
- [43] Saurabh Singh, Sami Abu-El-Haija, Nick Johnston, Johannes Ballé, Abhinav Shrivastava, and George Toderici. End-to-end learning of compressible features. In *ICIP*, 2020.
- [44] George Toderici, Damien Vincent, Nick Johnston, Sung Jin Hwang, David Minnen, Joel Shor, and Michele Covell. Full resolution image compression with recurrent neural networks. *Proceedings - 30th IEEE Conference on Computer Vision and Pattern Recognition, CVPR 2017, 2017-January*:5435–5443, 2017.
- [45] Robert Torfason, Fabian Mentzer, Eirikur Agustsson, Michael Tschanen, Radu Timofte, and Luc Van Gool. Towards image understanding from deep compression without decoding. *ICLR*, pages 1–17, 2018.
- [46] Matej Ulicny and Rozenn Dahyot. On using cnn with dct based image data.
- [47] Xin Wang, Thomas E Huang, Trevor Darrell, Joseph E Gonzalez, and Fisher Yu. Frustratingly simple few-shot object detection. *arXiv preprint arXiv:2003.06957*, 2020.
- [48] Yu-Xiong Wang, Deva Ramanan, and Martial Hebert. Meta-learning to detect rare objects. In *Proceedings of the IEEE International Conference on Computer Vision*, pages 9925–9934, 2019.
- [49] Xiaopeng Yan, Ziliang Chen, Anni Xu, Xiaoxi Wang, Xiaodan Liang, and Liang Lin. Meta r-cnn: Towards general solver for instance-level low-shot learning. In

Proceedings of the IEEE International Conference on Computer Vision, pages 9577–9586, 2019.

- [50] Amir R Zamir, Alexander Sax, William Shen, Leonidas J Guibas, Jitendra Malik, and Silvio Savarese. Taskonomy: Disentangling task transfer learning. In *Proceedings of the IEEE Conference on Computer Vision and Pattern Recognition*, pages 3712–3722, 2018.

APPENDIX A

APPENDIX I: COMPRESSION MODEL DETAILS

A.1 A Quantized Conditional Gaussian Model

Here we provide some more insight into the probabilistic model used for the arithmetic coding of the quantized compressible representation \hat{z} . We view this tensor as simply a list of N elements, where each element is an instance of random variable unique to that element. This means that the probabilistic model over the whole representation can be formalized as

$$p_{\hat{z}}(\hat{z}) = \prod_{i=1}^N p_{z_i}(\hat{z}_i) \quad (7)$$

Each element \hat{z}_i is modelled by an independent Gaussian with its own mean μ_i and its own standard deviation σ_i . Both of these parameters are obtained by decoding \hat{h} using the *hyper-decoder* network as discussed above. We use additive uniform noise to simulate quantization. We can formalize the density function \hat{z} as the following.

$$p_{z_i}(\hat{z}_i) = F_{\mathcal{N}}\left(\hat{z}_i + \frac{1}{2} \middle| \mu_i, \sigma_i\right) - F_{\mathcal{N}}\left(\hat{z}_i - \frac{1}{2} \middle| \mu_i, \sigma_i\right) \quad (8)$$

The cumulative function of a single variable Gaussian is known analytically if both the mean and the variance are known, which is the case here, so it can be used directly.

To better illustrate the *Conditional Gaussian model*, we take the example of an element of z valued at 3.25. The corresponding quantized value is 3. To arithmetically encode this value we need a probabilistic model over the integers. The hyper-prior network predicted this number with a Normal distribution with a mean of 4 and a variance of 1. It is not perfect, because the mean could be better and the variance lower. The continuous density function is presented by the blue line in figure 4. To obtain a probability mass function we apply Equation (8) to each of the integers. This is represented by the Diracs in the same image. In practice, we do not track the probabilistic mass of all the integers but only a small subset of them, specifically the one above a very low hyper-parameter value.

A.2 Hierarchical Variational Auto-Encoder

Now that all the different parts of the compression architecture are defined, we can describe how to actually train them.

In the univariate case, the added quantization noise around a value can be modelled as uniform density model with the input as the middle point and the quantized representation as a sample from that distribution. We also model each element of the quantized latent representation (\hat{z}, \hat{h}) as independent, meaning that the density function of

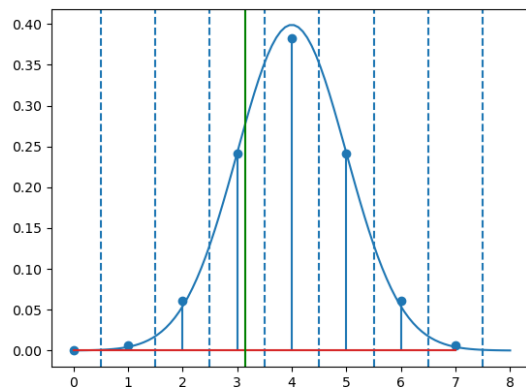


Fig. 4: Probability model used for an element of the latent representation if the associated gaussian has a mean of 4 and variance of 1. The key point is that this leads to a latent continuous representation that can be easily quantized into integers in the interval $[0, 7]$.

the whole density distribution is given by multiplying the density function of all the elements. The resulting density function, given by Equation (9), is uniformly distributed in the unit hypercube around the point (z, h) resulting in the processing of a given x .

$$q(\hat{z}, \hat{h}|x) = \prod_i \mathbb{1}_{[\hat{z}_i - \frac{1}{2}, \hat{z}_i + \frac{1}{2}]} \prod_j \mathbb{1}_{[\hat{h}_j - \frac{1}{2}, \hat{h}_j + \frac{1}{2}]} \quad (9)$$

The way to train this density function is to minimize the KL divergence between $q(\hat{z}, \hat{h}|x)$, the learned density function of the quantized representation (\hat{z}, \hat{h}) and the probabilistic model over it. This is formalized as

$$KL[q \| p_{z,h|x}] = \mathbb{E}_q \left[\log \frac{q(\hat{z}, \hat{h})}{p(z, h|x)} \right] \quad (10)$$

This can be reduced to

$$KL[q \| p_{z,h|x}] = -\mathbb{E}_q[\log p(x|\hat{z}, \hat{h})] + KL[q \| p_{\hat{z}, \hat{h}}] \quad (11)$$

This resulting objective function is the same as the usual VAE objective. To be more precise, it can be seen a Hierarchical Variational Auto-Encoder and (\hat{z}, \hat{h}) , can be seen as a sample of the latent representation of the model. In this view, quantization is equivalent to sampling. This is very similar to the well known “reparameterization trick” used for VAEs. The resulting computation graphs for this reparameterization technique are shown in Figure 5, where $q(\hat{z}, \hat{h}|x)$ is the learned density function of the quantized latent representation, which is an approximation of the true posterior $p(\hat{z}, \hat{h}|x)$.

Equation 11 can further be modified to obtain the following form:

$$KL[q \| p_{z,h|x}] = \|\hat{x} - x\|^2 + E_q[-\log p(\hat{z}|\hat{h})] + E_q[-\log p(\hat{h})] \quad (12)$$

where $E_q[-\log p(\hat{h})]$ is the expected compression rate using entropy coding of \hat{h} when the univariate density model is used as the probabilistic model and $E_q[-\log p(\hat{z}|\hat{h})]$ is the expected compression rate using entropy coding of \hat{z} when

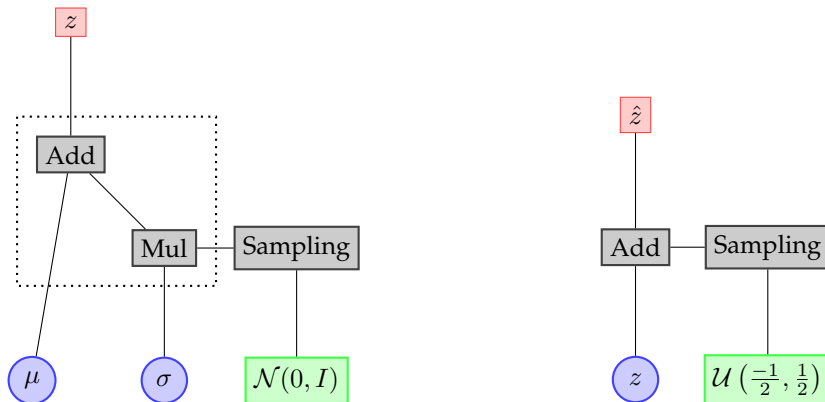


Fig. 5: (left) Computation graph for the sampling procedure used for the reparameterization trick with a Gaussian distribution. (right) Computation graph for the additional use of additive uniform noise to simulate quantization.

the Conditional Gaussian model is used as the probabilistic model. Equation (12) is not a compression loss because the trade-off between compression and image fidelity cannot be adjusted. So it is modified into the following equation

$$\lambda \|\hat{x} - x\|^2 + E_q[-\log p(\hat{z}|\hat{h})] + E_q[-\log p(\hat{h})] \quad (13)$$

In this formulation we can easily see the distortion term $\|\hat{x} - x\|^2$ and the rate terms $E_q[-\log p(\hat{z}|\hat{h})] + E_q[-\log p(\hat{h})]$. This formulation is equivalent to the β -VAE [22] which has been shown to lead to more disentangled representations, making such representations even more useful as features for other tasks because new tasks could focus on specific features to accomplish specific objectives.

A.3 Architecture

A.3.1 Image Compression framework

This encoder is composed of four convolutional layers interlaced by Generalized Divisive Normalization (GDN) layers [3] as activation functions. It was inspired by Divisive Normalization (DN) [8] which is a multivariate non-linearity designed to model the responses of sensory neurons in biological systems, and it was shown to play a role in efficient information processing. It is defined as:

$$z_i = \frac{x_i}{(\beta_i + \sum_j \gamma_{ij} |x_j|^{\alpha_{ij}})^{\epsilon_i}} \quad (14)$$

where x_i and z_i denote the input and output vectors. The parameters α_{ij} , β_i , γ_{ij} and ϵ_i are trainable parameters. i is the index of the element on which the activation function is computed and j is the index of elements in the neighbourhood of element x_i . The neighbourhood is the receptive field of a convolution operation. It has been shown that in practice, GDN, compared to common pointwise activation functions such as relu or tanh, yields better performance at the same number of hidden units and comes with a negligible increase in number of model parameters when used in an image compression pipeline using neural networks [3]. The decoder uses the Inverse Generalized Divisive Normalization (IGDN) and it is defined as :

$$z_i = x_i (\beta_i + \sum_j \gamma_{ij} |x_j|^{\alpha_{ij}})^{\epsilon_i} \quad (15)$$

It uses the same operation as the GDN, but instead of dividing by the normalization factor, it multiplies by it. This is seen as doing the inverse work of the GDN, this is why it is used in the image decoder because it does the inverse function of the encoder. We used the same simplifications in the IGDN as the ones we used for the GDN, when it was used in the image decoder.

The encoder expects an RGB image of size $3 \times W \times H$ and outputs a tensor of shape $256 \times W/16 \times H/16$. Note, the rank of the compressible format is a third of the input rank and is still much smaller than the input (in bits/pixel) because of its smaller spatial resolution and redundancy. The actual architecture of the encoder and the image decoder are presented in the Table 5. In this table, *Conv* represents a convolution layer where k represents the kernel size, c represents the amount of output channels and s represent the stride. We use the stride to do the downsampling instead of using a pooling operation. *TConv* is a transposed convolution, it is used to upsample the representation.

Encoder	Image Decoder	Hyper-Encoder	Hyper-decoder
Conv : 5k, 256c, 2s	TConv: 5k, 256c, 2s	Abs	TConv 5k, 256c, 2s
GDN	IGDN	Conv : 3k, 256c, 2s	Leaky ReLU
Conv : 5k, 256c, 2s	TConv: 5k, 256c, 2s	LeakyReLU	TConv 5k, 384c, 2s
GDN	IGDN	Conv : 5k, 256c, 2s	Leaky ReLU
Conv : 5k, 256c, 2s	TConv: 5k, 256c, 2s	LeakyReLU	TConv 5k, 512c, 2s
GDN	IGDN	Conv : 5k, 256c, 2s	
Conv : 5k, 256c, 2s	TConv: 5k, 3c, 2s		

TABLE 5: Architecture of the modules used in the compression framework

A.3.2 Resnet

The Resnet-101 is used as a baseline backbone for the different vision downstream tasks when going from the RGB images. We present, in detail, on Table 6 the truncated-resnet architecture, used by [45] as compared to the original resnet and our proposed SubPixel variation.

A.3.3 Truncated-Resnet

When going from the compressible representation, we want to use a backbone architecture that is similar in design and complexity to the Resnet-101 backbone. The first architecture that we used is the architecture we call the Truncated-Resnet. We cannot use the Resnet stem, which are the first

Block name	Resnet	Truncated Resnet	SubPixel Resnet
Stem	$\begin{bmatrix} 7 \times 7, 64, \text{stride } 2 \\ 3 \times 3, \text{MaxPool}, \text{stride } 2 \end{bmatrix}$	-	$\begin{bmatrix} \text{Block}(256, 64) \\ \text{PixelShuffle}(2) \\ \text{Block}(64, 16) \\ \text{PixelShuffle}(2) \\ \text{Block}(16, 16) \\ 1 \times 1, 64 \end{bmatrix}$
layer2	$\begin{bmatrix} 1 \times 1, 64 \\ 3 \times 3, 64 \\ 1 \times 1, 256 \end{bmatrix} \times 3$	-	$\begin{bmatrix} 1 \times 1, 64 \\ 3 \times 3, 64 \\ 1 \times 1, 256 \end{bmatrix} \times 3$
layer3	$\begin{bmatrix} 1 \times 1, 128 \\ 3 \times 3, 128 \\ 1 \times 1, 512 \end{bmatrix} \times 4$	$\begin{bmatrix} 1 \times 1, 512 \\ 1 \times 1, 128 \\ 3 \times 3, 128 \\ 1 \times 1, 512 \end{bmatrix} \times 2$	$\begin{bmatrix} 1 \times 1, 128 \\ 3 \times 3, 128 \\ 1 \times 1, 512 \end{bmatrix} \times 4$
layer4	$\begin{bmatrix} 1 \times 1, 256 \\ 3 \times 3, 256 \\ 1 \times 1, 1024 \end{bmatrix} \times 23$	$\begin{bmatrix} 1 \times 1, 256 \\ 3 \times 3, 256 \\ 1 \times 1, 1024 \end{bmatrix} \times 23$	$\begin{bmatrix} 1 \times 1, 256 \\ 3 \times 3, 256 \\ 1 \times 1, 1024 \end{bmatrix} \times 23$
layer5	$\begin{bmatrix} 1 \times 1, 512 \\ 3 \times 3, 512 \\ 1 \times 1, 2048 \end{bmatrix} \times 3$	$\begin{bmatrix} 1 \times 1, 512 \\ 3 \times 3, 512 \\ 1 \times 1, 2048 \end{bmatrix} \times 3$	$\begin{bmatrix} 1 \times 1, 512 \\ 3 \times 3, 512 \\ 1 \times 1, 2048 \end{bmatrix} \times 3$

TABLE 6: Resnet Architectures. We compare the original Resnet for full scale images (left), with the Truncated Resnet [45] and our SubPixel resnet used on the main results of the paper.

high kernel size convolution blocks on the Resnet architecture. The compressible input is of a different dimensionality and is not compatible with the Resnet backbone. Based on the architecture used in [19], we adapt the Resnet backbone by removing the stem, layer 1 and the first two residual blocks of layer 2. The reason we chose to remove those layer is that the spatial resolution of the tensor at this point of the Resnet network matches the spatial resolution of the compressible representation. To match the number of feature maps of the tensor expected at this point in the Resnet architecture, we add a 1×1 convolutional layer to increase the number of feature maps of the compressible input format. We do not change at all the layers 3 and 4 of the Resnet architecture. This way, the number of parameters in the original Resnet architecture and the truncated architecture is very similar, and most of the architecture is the same. This makes it fair to compare performance metrics on the different vision tasks when going from images versus when going from the compressible representation.

A.3.4 SubPixel-Resnet

In order to improve on the Truncated-Resnet architecture we develop a subpixel variant. In this new architecture, we keep the layers 1 to 4 the same as in the Resnet architecture, but we propose a new stem that is more adapted to the compressible representation as input. This way, this architecture is mostly the same as the original Resnet architecture, making comparison between them fair.

First, the expected output tensor spatial dimensionality of the Resnet stem is 4 times smaller than the input image. Our compressible representation has a spatial dimensionality that is 16 times smaller than the input image, which means that we need the output representation of the Sub-Pixel Stem must be four times greater than the ones of the compressible representation. The usual solution in this case is to use a deconvolution operation. We instead chose to use the pixel-shuffle operation followed by convolutions. This operation is recent and was originally proposed in the context of single image super resolution (SISR). The goal of that research was to produce a high-resolution image

from a low-resolution input and they achieved state-of-the-art results at the time [42]. The process is shown in figure 6 and is called a sub-pixel convolution when it is followed by a convolution operation. The way it works is by moving the

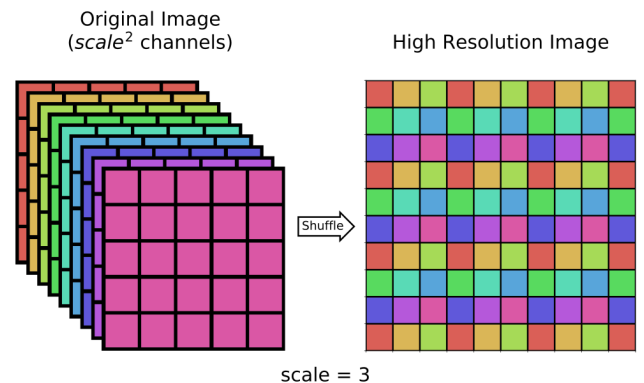


Fig. 6: Pixel Shuffle operation with a scale of 3

low-resolution channels into the spatial dimension to create an image with a higher spatial resolution. This is a more efficient transformation than the transposed convolution operation. It does not increase the receptive field, this is why it called a sub-pixel convolution. Also, it has been shown [9], that the sub-pixel convolution has a better than the deconvolution. The deconvolution creates checkerboard artifacts in a multitude of tasks when it is used to increase the spatial resolution. To alleviate this checkerboard problem a solution that was used what to upsample the representation using bicubic interpolation and then do a convolution. The sub-pixel convolution does not create checkerboard artifacts and replaces the up-sampling steps. We separate the 4 times spatial up-sampling in two separate operations that will each up-sample by a factor of two. This is done, because preliminary results showed that it was yielding better performance.

Second, we change the convolution in the original stem with a custom residual block, similar to the one used in Resnet architecture, but only composed of convolutional layers with a kernel of size 3. The three consecutive convolu-

tions with kernel size of 3 have the same receptive field as a single convolution layer with a kernel of 7. This replaces the convolution in the stem of the original Resnet architecture, while having fewer parameters. This type of replacement has been shown to improve performance in vision tasks both in performance metrics and in speed. The normalization function we used is batch normalization.